

Breakthrough and thermodynamic adsorption of Cr (VI) y Ni (II) bioadsorption in continuous system

Curva de ruptura y termodinámica de la bioadsorción de Cr (VI) y Ni (II) en sistema continuo

C. Tejada-Tovar  ; L. C. Newball-López  ; C. E. Cardona-Lara 

DOI: <https://doi.org/10.22517/23447214.23341>

Artículo de investigación científica y tecnológica

Abstract—The removal of heavy metals present in water is an issue of environmental interest, due to bioaccumulation, biomagnification and the carcinogenic and mutagenic effects on living beings. The objective of the present study was to use plantain peel residues in Chromium (VI) and Nickel (II) removal in continuous system, evaluating the effect of bed height, temperature and adsorbent particle size on the process; obtaining a 98.7% 99.71% removal yield for Cr (VI) and Ni (II), respectively. The FTIR showed that the bioadsorbent has a heterogeneous structure with the presence of hydroxyl groups, saturated and unsaturated hydrocarbons, carbonyls, carboxyl, among others, and it was established that the process is controlled by electrostatic reactions between the active centers and the metal. The breakage curve was carried out under the optimal conditions established by the Response Surface Methodology (RSM) and it was established that the bioadsorbent has an extensive useful life, as it was not saturated throughout the process. The thermodynamic parameters established that the process is exothermic and irreversible, being favored at room temperature. Taking into account the behavior of plantain peels during the breakage curve, it is recommended to use it as a filler in a packed bed to remove Cr (VI) and Ni (II).

Index Terms—Adsorption; heavy metals; fixed bed; lignocellulosic biomass; plantain peels.

Resumen—La remoción de metales pesados presentes en aguas es un tema de interés ambiental, debido a la bioacumulación, biomagnificación y los efectos cancerígenos y mutagénicos para los seres vivos. El objetivo del presente estudio fue usar residuos de cáscara de plátano en la remoción de Cromo (VI) y Níquel (II) en sistema continuo, evaluando el efecto de la altura del lecho, temperatura y tamaño de partícula del adsorbente sobre el proceso; Obteniendo un

This manuscript was sent on February 02, 2020 and accepted on February 05, 2021.

C. Tejada-Tovar, L. Newball, and C. Cardona are researchers for the Process Design and Biomass Utilization Research Group (IDAB) at Facultad de Ingeniería at Universidad de Cartagena. Cartagena, Zip code: 130015, Colombia (they e-mail are: *ctejadat@unicartagena.edu.co, lnewball@unicartagena.edu.co, ccardonal@unicartagena.edu.co, respectively). and *Correspondence author

rendimiento en la remoción del 98,7% 99,71% para Cr (VI) y Ni (II), respectivamente. El FTIR mostró que el bioadsorbente tiene una estructura heterogénea con presencia de grupos hidroxilo, hidrocarburos saturados e insaturados, carbonilos, carboxilo, entre otros, y se estableció que el proceso es controlado por reacciones electrotácticas entre los centros activos y el metal. La curva de ruptura se realizó a las condiciones óptimas establecidas por la Metodología Superficie Respuesta (RSM) y se estableció que el bioadsorbente tiene una vida útil extensa, en tanto no se saturó a lo largo del proceso. Los parámetros termodinámicos establecieron que el proceso es exotérmico e irreversible, viéndose favorecido a temperatura ambiente. Teniendo en cuenta el comportamiento de las cáscaras de plátano durante la curva de ruptura, se recomienda su uso como relleno en un lecho empacado para remover Cr (VI) y Ni (II)

Palabras claves— Adsorción; Biomasa lignocelulósica; Metales pesados; lecho empacado; cáscaras de plátano

I. INTRODUCTION

CONTAMINATION of water sources by Cr(VI) and Ni(II) is an environmental problem, due to its harmful effects on health and ecosystems [1], [2]. Chromium causes respiratory problems, lung cancer and affects the male reproductive system [3], [4]. For its part, chromium is dumped into the environment in effluents from the fertilizer, textile, photographic, pigment, tannery, electroplating, and electronic manufacturing industries, among others [5], and in its oxidation +6 state it crosses biological barriers, with carcinogenic and mutagenic effects [6], [7]. Nickel is widely used in production of batteries, steel, alloys, and prolonged exposure to it can cause stomach aches and carcinogenic effects on the blood, kidneys, or chronic bronchitis and alteration of the lung [3].

These metals are bioaccumulative, are magnified in the food chain and are resistant to degradation [8]; therefore, different techniques have been implemented for the removal of heavy metals in solution such as: oxidative techniques, filtration and ultrafiltration, membrane extraction, ion exchange, among others [9], [10]. However, the application of these technologies is expensive due to operational and energy costs,

labor; in addition, they generate toxic waste sludge and have little efficiency at trace concentration levels [11].

Bioadsorption is presented as an alternative for the removal of heavy metals present in wastewater, due to the high adsorption capacity that lignocellulosic adsorbents present, the low cost, availability, and reuse of the raw material [12], [13]. Thus, different agricultural and agroindustrial biomasses have been used in the removal of heavy metals such as: lychee [14], grapefruit [15], pineapple and orange [16], lime [17], coffee waste [8], yucca and yam [18], bagasse [19], among others [20]–[23]. So, the objective of this research was to establish the effect of temperature, bed height and particle size in Ni (II) and Cr (VI) biosorption on plantain peel in a continuous system, determining the optimal operating conditions through the Response Surface Methodology and the bed saturation time.

II. MATERIALS AND METHODS

A. Materials and reactives

To prepare the solutions, Merck brand Nickel Sulfate (NiSO_4) and Potassium Dichromate (HCrO_7) were used. To adjust the pH, solutions of 1M Sodium Hydroxide (NaOH) and Hydrochloric Acid (HCl) were used. The FTIR in a NICOLET 6700. The solutions were prepared using deionized water.

B. Design of experiments

An experimental design known as central star composite response surface was used with the objective of not making replicas (Table I), in which the effect of three factors was analyzed: temperature, particle size and bed height; which were worked with five levels of variation each.

TABLA I.
RANGES AND LEVELS OF VARIATION.

Independent variables	Indicator	Range and level				
		$-\alpha$	-1	0	+1	$+\alpha$
Particle size	mm	0.1351	1	0.5	0.355	1.2189
Bed height	mm	6.1373	30	65	100	123.863
Temperature	°C	29	40	55	70	80

C. Preparation and characterization of the adsorbent

The plantain peel, collected in sufficient quantity to perform all the experiments, was washed, dried by sun for three days and at 90 °C in an oven for 24 hours [4]. It was then reduced in size and sized in a shaker-type sieve, selecting mesh sizes of 0.1351, 0.355, 0.6775, 1 and 1.2198 mm [5]. The prepared adsorbent was characterized by FTIR analysis to identify the groups involved in the adsorption process [4].

D. Adsorption tests in continuous system

Adsorption tests of Cr (VI) and Ni (II) were performed at pH 2 and 6, respectively, and 100 ppm, following the

proposed experimental design; a continuous system equipment with acrylic columns of 4.1 cm internal diameter and height of 15 cm was used, with a flow rate between 11-15 mL/min [5]. The variation and control of the temperature was made by means of an Arduino nano controller. Samples to measure the final ion concentration in the solution were taken at the bottom outlet of the column. The final concentration of Ni (II) was determined by atomic absorption and the Cr (VI) concentration by UV-VIS spectrophotometry using the 1,5-diphenylcarbazide colorimetric method at 540 nm in a UV-Vis spectrophotometer model BK-UV 1900.

E. Statistical analysis.

The analysis of the results was carried out in the STATGRAPHICS Centurion 18.1.02 software, in order to optimize the process using the Response Surface Method (RSM) and to determine the incidence of the variables studied on the adsorption of Chromium (VI) and Nickel (II), using analysis of variance, Pareto diagram for each of the biomasses under study.

F. Breakage curve and fit to models

The breakage curve was made by placing Cr (VI) and Ni (II) contaminated solution in contact with the bioadsorbent, at the optimal conditions of temperature, particle diameter and bed height found by RSM for each contaminant. Adams-Bohart, Thomas, Yoon-Nelson and dose-response models were used to predict the column behavior, calculating the process constants and evaluating the adsorption capacity of the adsorbent.

G. Adsorption models used in the breakage curve

Adams-Bohart model

The Adams-Bohart model is used only for the initial description of the breakage curve above the breakage point or saturation points; it only describes between 10-50% of the behavior. It assumes that the adsorption rate is proportional to the adsorption capacity and the concentration of the adsorbed species [6].

This model is described according to (1):

$$\frac{C_o}{C} = \frac{\text{EXP}(K_{AB} C_o t)}{1 + \text{EXP}\left(\frac{K_{AB} N_o L}{v}\right) - 1 + \text{EXP}(K_{AB} C_o t)} \quad (1)$$

Where KAB is the kinetic constant of AB in (L/mg.min), NO is the maximum volumetric adsorption capacity in mg/L and v is the linear flow rate in (cm/min), L is the column bed depth in cm, CO is the internal concentration mg/L, Ct is the effluent concentration and t is the residence time of the solution in the column [7].

Thomas model

Thomas' model is of a dynamic type and follows Langmuir's adsorption kinetics. In this model the axial dispersion is considered to be negligible in the bed, due to the fact that the driving force obeys a second-order kinetics with a reversible reaction [8].

Given by (2):

$$\frac{C_o}{C} = \frac{1}{1 + EXP\left[\frac{K_{th}}{Q} (q_o X - C_o V)\right]} \quad (2)$$

Where K_{th} , is the Thomas constant ($\text{mL}/\text{min}^{-1} \text{mg}^{-1}$); q_o , is the maximum solute concentration in the solid phase (mg/g); X , is the amount of adsorbent in the column (g), Q is the flow rate (mL/min) and V (L) is the volume of the effluent at the time of operation [9].

Dose-Response Model

The Dose-Response model has been commonly used in pharmacology to describe different types of processes, and is currently being applied to describe columnar biosorption [24]. The DR model can be represented by (3):

$$\frac{C_o}{C} = 1 - \frac{1}{1 + \left[\frac{C_o * Q t}{q_o X}\right]^a} \quad (3)$$

Where a is the model constant, q_0 , maximum solute concentration in the solid phase (mg/g), X , is the amount of adsorbent in the column (g) and Q is the flow rate (mL/min) [25].

H. Calculation method of the total amount of metal removed

The amount of metal removed for PP-Cr(VI) was resolved by calculating the area under the breakage curve using the following integral shown in (4) and (5):

$$q_e = \frac{Q}{1000} \left(\int_0^{10} (C_i - C_o) dt + \int_{10}^{30} (C_i - C_o) dt + \int_{30}^{60} (C_i - C_o) dt + \int_{60}^{120} (C_i - C_o) dt + \int_{120}^{1020} (C_i - C_o) dt \right) \quad (4)$$

And for PP-Ni(II) was used:

$$q_e = \frac{Q}{1000} \left(\int_0^{10} (C_i - C_o) dt + \int_{10}^{30} (C_i - C_o) dt + \int_{30}^{60} (C_i - C_o) dt + \int_{60}^{180} (C_i - C_o) dt + \int_{180}^{300} (C_i - C_o) dt + \int_{300}^{420} (C_i - C_o) dt + \int_{420}^{540} (C_i - C_o) dt + \int_{540}^{600} (C_i - C_o) dt + \int_{600}^{720} (C_i - C_o) dt \right) \quad (5)$$

The numerical integration was done by the Simpson 1/3 method and the different integrals are done for the reason that the separation of all the points are not equidistant so it is done by intervals which certainly are. The total amount that passes through the column, the percentage retained, the biosorption capacity and the metal in solution at the end are calculated by (6) to (9):

$$m_{total} = \frac{C_i Q t_{total}}{1000} \quad (6)$$

$$\% \text{ retained} = \frac{q_{total}}{m_{total}} * 100 \quad (7)$$

$$q_e = \frac{q_{total}}{m} \quad (8)$$

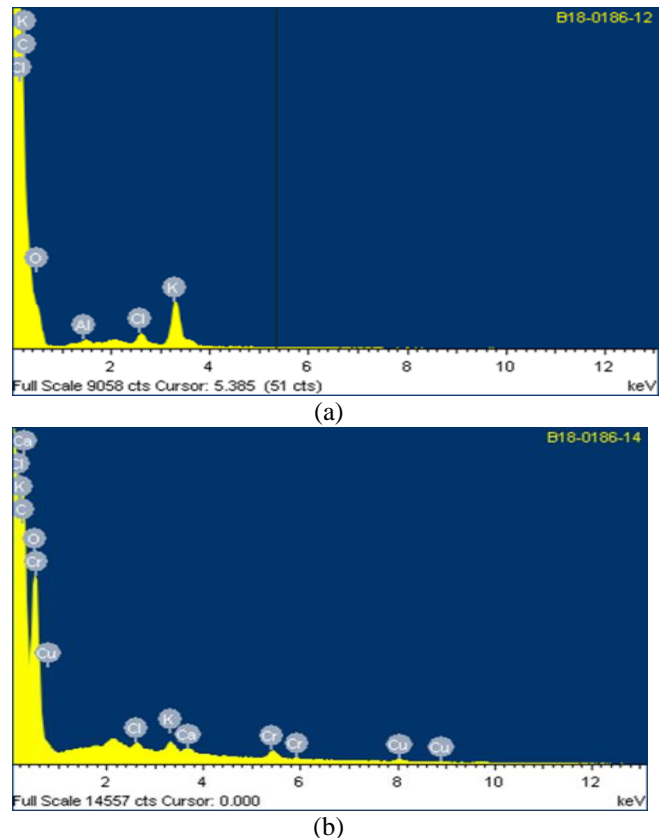
$$C_e = \frac{m_{total} - q_{total}}{Q * t_{total}} * 1000 \quad (9)$$

III. RESULTS AND DISCUSSION

A. Adsorbent characterization

The adsorption process is a complex multi-step phenomenon that involves many factors; among these, the surface chemistry and pore structure of the biomasses studied are influential. In Fig. 1a, it is shown the spectrogram obtained and the chemical composition in % of atomic weight for unsaturated PP, and after the removal of Chromium (VI) (Fig. 1b) and Nickel (II) (Fig. 1c). It was obtained that carbon and oxygen are the most present in all the materials studied, with 75.18 and 23.34%, respectively, which can be attributed to their organic nature; as well as elements in small proportions: Al, Cl and K [2], [26]. De igual forma, después del proceso de remoción, se evidencia la presencia de los iones metálicos removidos.

Fig. 2a shows the scanning electron microscopy (SEM) images of the PP, which has a cylindrical agglomerated appearance.



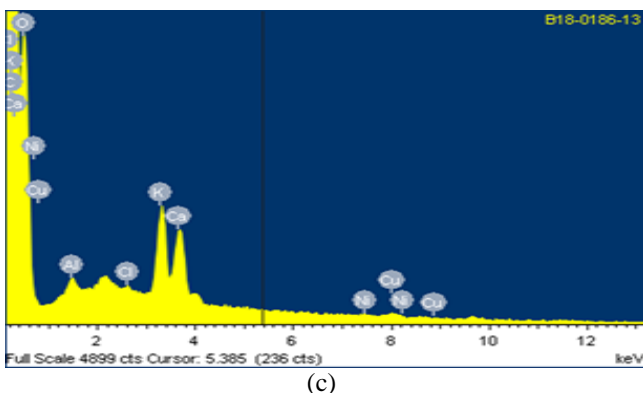


Fig. 1. EDS analysis of unsaturated plantain peel (a) and after the adsorption process of Chromium (b) and Nickel (c).

From SEM micrographs after the adsorption experiments it was found that Cr (VI) and Ni (II) ions were adsorbed on the plantain peel biomass surface according to an electrostatic attraction mechanism, suggesting that the process is dominated by chemisorption [26], [27].

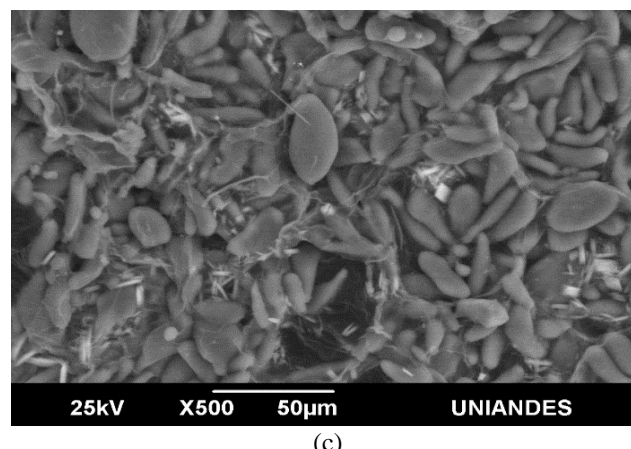
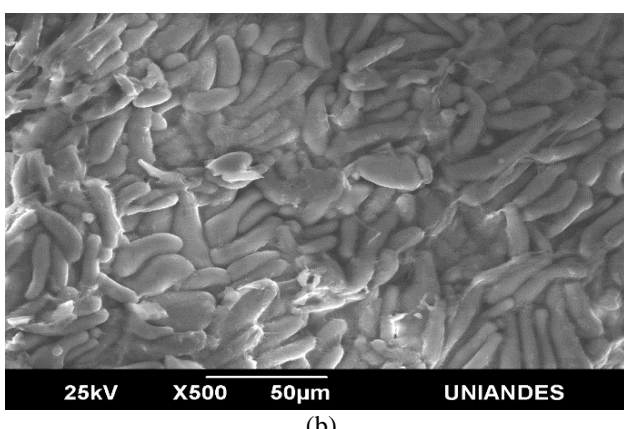
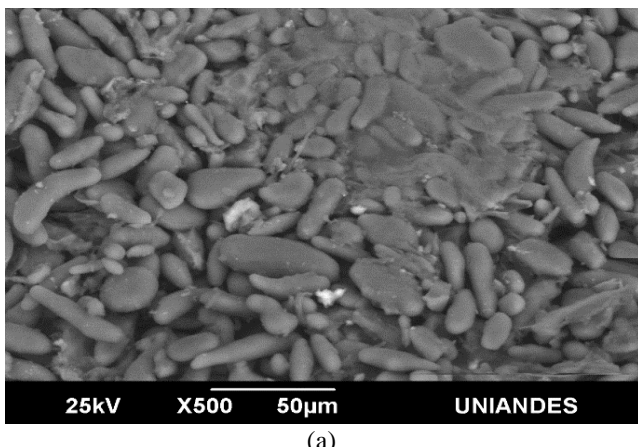


Fig. 1. SEM microphotographs of unsaturated plantain peel (a) and after the adsorption process of Chromium (b) and Nickel (c).

FTIR analysis of biomass provides information regarding the organic functional groups present inside the structure of the lignocellulosic material, which have been reported as participants in ion exchange to capture the contaminant within the pores of the biosorbent [28]–[30]. Fig. 3 shows the IR spectrum of the PP before and after the Cr (VI) and Ni (II) removal process, and shows the representative peaks corresponding to the vibration and stretching of the OH, C-H, C=O, COOH groups [31], [32].

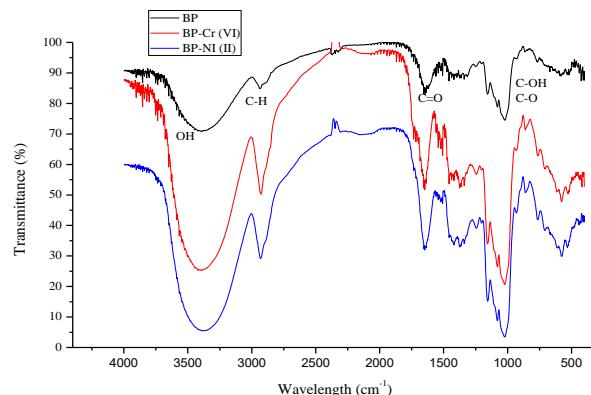


Fig. 2. FTIR plantain peel (PP) before and after the adsorption process of Cr (VI) and Ni (II).

From the spectrum of Fig. 3, a broadband at 3387 cm⁻¹ is identified due to the characteristic vibration of the O-H hydroxyl present in the hydrocarbon chains of cellulose, hemicellulose and lignin present in the material [33]–[35]. The fluctuation in 2931 cm⁻¹ is due to the C-H bond or aliphatic group resulting from the organic compound structure in the material structure attributed to the possible presence of methyl, methylene or methoxy groups [36], [37]. The peak at 1652 cm⁻¹ is an indication of carbonyl groups, possibly a result of the carboxylic groups of pectin, hemicellulose and lignin [38]. The frequency observed between 1010-1419 cm⁻¹ can be attributed to the vibration of carboxylic acids and alcohols [30].

After the adsorption process a noticeable change in the spectrum of both biomaterial samples is observed, showing stretching of the bands at certain frequencies compared to the unused biomaterial. The vibrations of the

hydroxyl, carbonyl, alcoholic, aliphatic and carboxyl groups are much more pronounced; these changes can be attributed to the metal presence, both Ni (II) and Cr (VI), in the structure of the biomaterial which is the result of the union of the metals to the different functional groups [33].

B. Adsorption tests of Cr (VI) and Ni (II)

Table II presents the results obtained in each adsorption test, according to the experimental design previously raised. From the results, it is observed that the PP showed

a good performance in the removal of Cr (VI), reaching percentages between 90 % - 98.7 %; good results were also obtained in the removal of Ni (II), reaching percentages of removal higher than 70 % below all the conditions evaluated. This is due to the presence of carbonate compounds in the structure of the biomaterial, which suggests high presence of lignin and cellulose. The high removal efficiencies are also attributed to the presence of H- ions at the pH worked, which could contribute to the selectivity of the active centers by the metal [31].

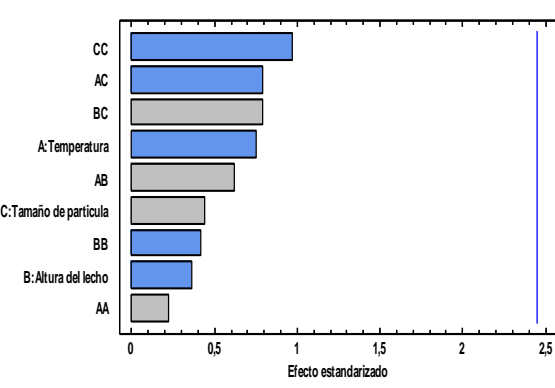
TABLA II.
REMOVAL PERCENTAGES OF CR (VI) AND NI (II) USING PP.

Temperature (°C)	Bed height (mm)	Particle size (mm)	Cr(VI) (%)	PP-Ni(II) (%)
55	65	0,6775	98,07	84,773
80,22	65	0,6775	97,45	90,836
55	6,13	0,6775	98,7	81,329
55	65	0,135122	89,32	99,354
40	100	0,355	97,75	99,714
40	100	1	97,82	92,329
55	65	1,219	98,7	85,419
70	30	0,355	98,7	94,854
55	65	0,677	98,07	84,773
40	30	1	97,82	74,698
29,77	65	0,677	98,7	85,978
70	30	1	90,57	73,388
70	100	1	96,95	77,255
55	123,8	0,677	93,07	75,706
70	100	0,355	97,82	98,962
40	30	0,355	98,7	94,406

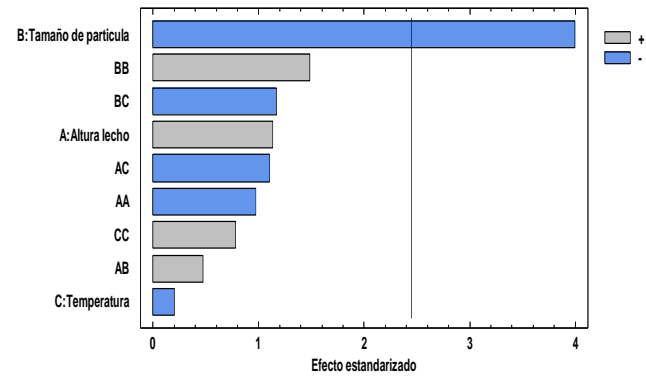
C. Effect of particle size, bed height and temperature on the % removal of Cr(VI) and Ni(II)

From Fig. 4a it can be said that none of the variables and their possible combinations in the experimental range established in the design of experiments reach 95% reliability, so they do not have a significant effect on the Cr (VI) removal, presenting the combination of

temperature-particle size a negative effect on the system as well as the temperature and height of the bed, as evidenced in the effects graph (Fig. 5a). The Pareto diagram for the removal of Ni (II) (Fig. 4b), shows that the variable that has the greatest influence within the system is the particle size, which determines the internal surface area and the number of sites available in the bioadsorbent [11], with temperature being the variable that has the least influence on the process.



(a)

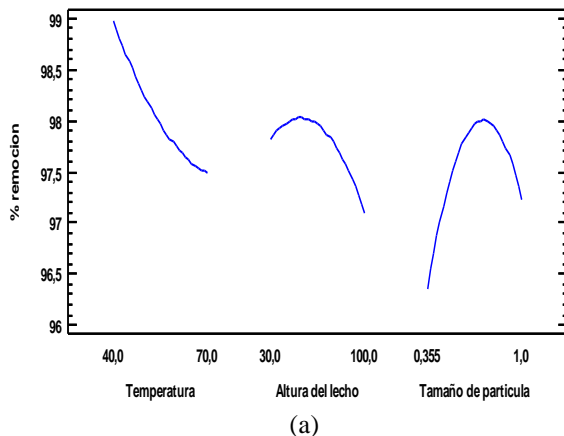


(b)

Fig. 3. Standardized Pareto diagram for the removal process of (a) Cr(VI) and (b) Ni(II).

Fig. 5 relates the variables together with the removal percentage. This graph allows us to understand the

behavior and effect that the controllable variables have on the system.

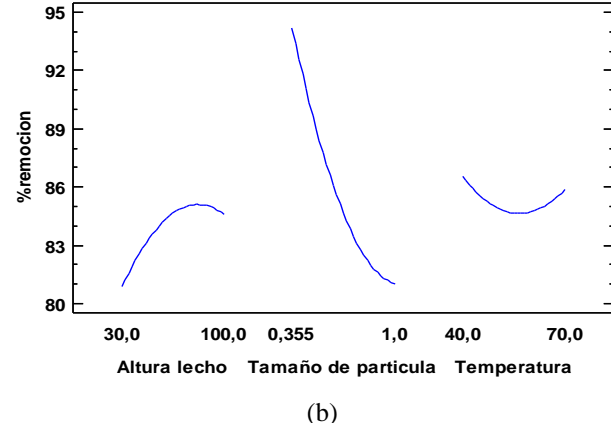


(a)

Fig. 4. Effect of temperature, bed height and particle size on the % removal of (a) Cr (VI) and (b) Ni (II).

From Fig. 5, it is established that increasing the solution temperature of the biomaterial throughout the evaluated range reduces the removal of Cr (VI), while for Ni (II) the decrease occurs from 40 to 50, which would imply a process of exothermic nature, which releases energy when the bonds between the contaminants with the functional groups are formed, and would indicate that the increase of energy in the system would cause a weakening of the interaction forces between the adsorbate and the adsorbent [39]–[41]. A temperature increase favors the desorption of the sorbate molecules over the biosorbent structure, because by gaining more energy than the bonds formed between the compounds support, the interaction forces are reduced, causing the release of what is not desired and this is a result of the temperature [42].

The increase of the bed height favors the adsorption due to the increase in the amount of active sites that allow the union of the ions with the functional groups, this effect is evident in the adsorption of Cr(IV) with bed heights between 30 and 56 mm; however for the heights of 56 to 100 mm when performing the experiment at high heights with low particle sizes the solution tended to seek the least tortuous path to descend along the bed, thus leaving areas without contact with the contaminated solution [43]. In contrast, the increase in the height of the bed favors proportionally the efficiency of NI (II) removal due to the fact that there is a greater biomass surface area because of the greater amount of particles; likewise, the diffusion phenomenon predominates over the axial dispersion phenomena in the mass transfer, causing an expansion of the mass transfer zone [44]. The good performance of Ni (II) removal can also be attributed to the availability of active contact sites between the metal and the particles, expanding the mass transfer zone by the higher mass transfer resistance and slower adsorption kinetics; in turn the increase in mass transfer resistance is caused by the repulsive forces between the adsorbed metals and the metals present in the solution bulk [45].



(b)

D. Optimization by Response Surface Methodology.

The optimal operating conditions for the adsorption system were obtained using the Response Surface Methodology (RSM), and are shown in Table III:

Conditions	SELECTED OPTIMAL VALUES FOR Ni(II) AND Cr (VI) ADSORPTION	
	Ni (II)	Cr (VI)
Temperature (°C)	29	29.8
Particle size (mm)	0.5	56.6
Bed height (mm)	110	1.0817

The predictions provided by the RSM for Cr (VI) are shown in the function graph as an estimated area (Fig. 6).

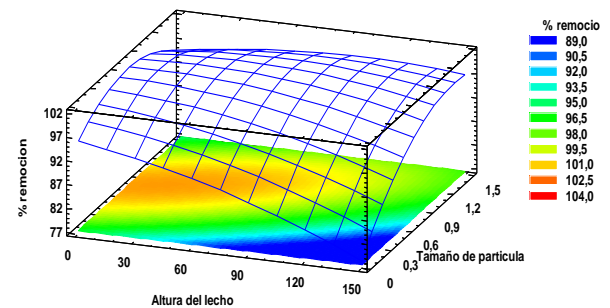


Fig. 5. Estimated response area for Cr (VI).

The temperature selected will be the ambient temperature because the system's behavior is more efficient when it is not supplied with energy.

The predictions for Ni (II) are shown in Fig. 7:

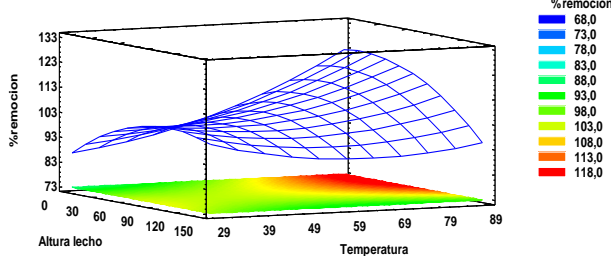


Fig. 6. Estimated response area for Ni (II).

E. Breakage curve modeling

The breakage curve of a bed makes it possible to establish its service life and saturation time [46]. Thus, the optimal bed height, particle size and temperature values, previously determined by the RSM, were used to achieve maximum removal in the adsorption tests. Fig. 8 shows the time vs C/C_i graph for Cr (VI) adsorption and Fig. 9 for Ni (II) adsorption, adjusted to Thomas, Response Dose, Yoon-Nelson, Adams-Bohart and BDST models [47].

The Cr (VI) breakage curve was made for approximately 17 hours, identifying the breakage time around of 300 min, where the output concentration was 7.3 ppm and therefore the removal percentage was 92.7%. The saturation point was determined at 1000 min with an output concentration of 69.4 ppm, which corresponds to 30% removal; and at 1020 min the system is considered to be in equilibrium, because the output concentration is 70 ppm. The behavior observed in the breaking curve, it can be said that the very low slope of the curve is due to the low concentration difference between the absorbent solution and the solute of the dissolution, creating a very low concentration gradient, resulting in a very weak driving force responsible for the transport of the contaminant from the fluid to the particle structure, which decreases the diffusion coefficient, causing the saturation time of the biomaterial to be much longer [48], [49].

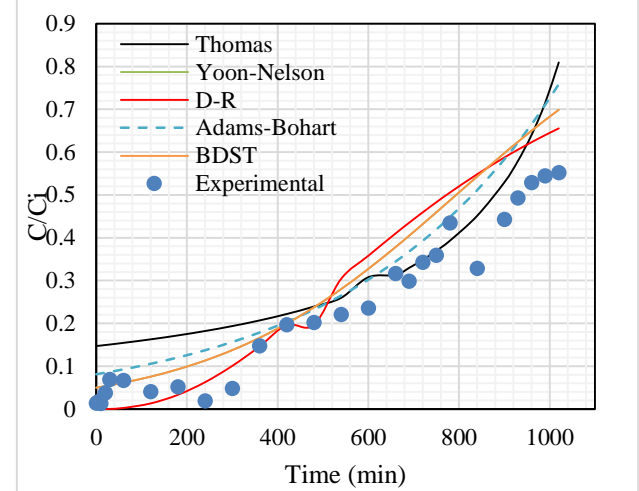


Fig. 7. Adjustment of Cr (VI) adsorption breakage curve to models.

The values of the system performance during the Cr (VI) and Ni (II) adsorption process are presented in Table IV, determining the amount of metal removed by calculating the area under the breakage curve using the x-equations, described in the methodology.

TABLA IV.
SYSTEM PERFORMANCE.

Parameters	Cr (VI)	Ni (II)
Total amount of metal (mg)	1530	354
Amount of metal removed (mg)	1054.1906	344.55
Percentage withheld (%)	68.901	97.33
Biosorption capacity (mg/g)	31.9452	5.8696
Metal in the solution (ppm)	31.098	12.304

Regarding the behavior of the Ni (II) breakage Curve, it can be seen that after 720 minutes of operation, it still presents a high removal capacity without reaching the breakage point. This could be due to the low volume of liquid that circulated through the column, which is represented by the value associated with the amount of metal fed into the column, which means that there would not be enough contaminant in the bed to come into contact with all the active sites of the biomass, causing the adsorption capacity of the biosorbent to be low in comparison with Cr (VI) [50], [51].

The adjustment parameters of the modeling of the breakage curves are presented in Table V.

TABLA V.
SETTING PARAMETERS OF CR (VI) AND NI (II) BREAKAGE CURVE MODELS.

Model	Parameter	Cr (VI)	Ni (II)
Thomas	K_{Th} (mL/min.mg)	0.0544444	0.0011
	q_0 (mg/g)	10.7506	366.4779
	R^2	0.9406	0.2015
Yoon-Nelson	K_{YN} (1/min)	0.0037	0.00042
	T (min)	793.7435	9726.4186
D-R	R^2	0.9843	0.1808
	A	2.3117	1.9549
	q_0 (mg/g)	25.7574	52.3808
Adams-Bohart	R^2	0.9798	0.0724
	K_{AB} (L/min.mg)	2.1948e-05	1.8283e-07
	N_0 (mg/L)	20711.2999	1210425.44
BDST	R^2	0.9768	0.20
	N_0 (mg/L)	13534.1924	1665816.8
BDST	K_{BDST}	3.723e-05	2.4175e-07

	(L/mg.min)	R ²
	0.9843	0.20

Observing the previous table, the models of best adjustment to the experimental data of Cr (IV) adsorption are Yoon-Nelson and BDST with an R² of 0.9843; nevertheless, the other models evaluated, also presented high R² values which indicate us that they are not so far from predicting the behavior of the breakage curve. However, when observing Fig. 8, the Thomas model moves considerably away from the experimental values at the beginning of the test, so this model is discarded from the analysis. With regard to Ni (II), the models evaluated did not adequately fit the experimental data due to the behavior that occurred in the bed. This behavior suggests the need to develop our own equations to describe the process and perform a correct industrial scaling.

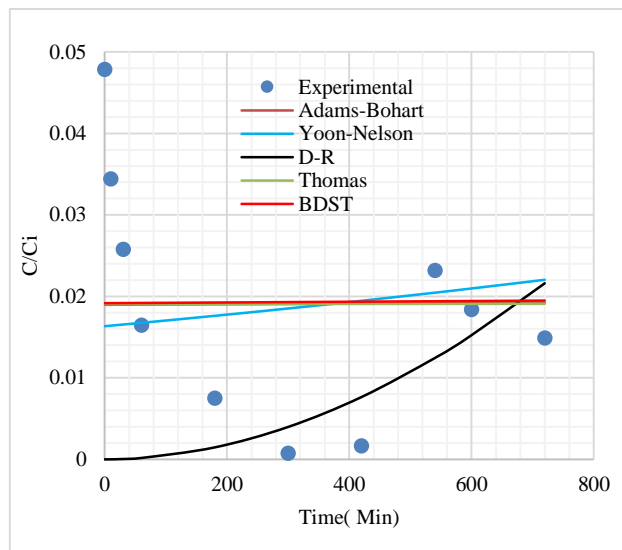


Fig. 8. Adjustment of Ni (II) adsorption breakage curve to models.

F. Thermodynamic parameters

Thermodynamic parameters reflected the feasibility and spontaneous nature of the process; thus, free energy change, enthalpy change and surface entropy change were estimated using the change of the equilibrium constant with absolute temperature [28]. For this, the Van't Hoff graphical method was used, which expresses the change in free energy as a function of the change in enthalpy and adsorption entropy with temperature, obtaining the regression line $-\Delta S^\circ$ and intercepting ΔH° as expressed in the equation [39]. The thermodynamic parameters for Cr and Ni(II) adsorption are shown in Table VI:

TABLA VI.
THERMODYNAMIC PARAMETERS FOR ADSORPTION OF Cr(VI) AND Ni(II).

T (K)	Cr (VI)			Ni (II)		
	ΔG° (kJ/mol)	ΔH° (kJ/mol)	ΔS° (kJ/molK)	ΔG° (kJ/mol)	ΔH° (kJ/mol)	ΔS° (kJ/molK)
303.15	393.6003	-225.6712	-2.0428	434.5156	-976.9138	1.7892
328.15	670.3412			-587.1284		
353.37	721.8604			-632.2522		

It is observed that Gibbs' energy in the Cr (VI) removal process increased proportionally with temperature, which corroborates the non-spontaneous increase of the removal. The negative direction of Entalpy in the removal of Cr(VI) and Ni(II) indicates the exothermic nature of the process, which is consistent with the results found above. On the other hand, the negative value of the Entropy of adsorption of both metals indicates a low reversibility in the process and a low randomness in the liquid-solid interface in the adsorption process [52], [53]. The decrease in the free energy of Gibbs during Ni(II) removal indicates that the spontaneity of the process is inversely proportional to the temperature increase, so the system does not need energy additions to react [54], [55].

IV. CONCLUSIONS

The use of plantain peel as a bioadsorbent for the removal of Cr(VI) and Ni(II) proved to be efficient. It was found in the FTIR analysis the presence of functional groups such as hydroxyl, carbonyl and carboxyl, which are attributed with affinity with the ions of heavy metals, participating in the adsorption, and the SEM-EDS analysis established that the adsorption is given by electrostatic forces inside the pores of the adsorbent. The behavior obtained in the breakage curve shows in turn the efficiency of the biomass and that the service time of the biomass is extensive, so it is recommended for implementation in packed beds to remove the metals under study. The thermodynamic parameters established that the adsorption process is exothermic, irreversible, and does not require the addition of energy for its operation.

ACKNOWLEDGMENTS

The authors thank the Universidad de Cartagena for the support to develop this research, laboratories, software and time of the research professors.

REFERENCES

- [1] S. Kulbir, W. S. Abdullahi, and R. Chhotu, "Removal of Heavy Metals by Adsorption using Agricultural based Residue: A Review," *Res. J. Chem. Environ.*, vol. 22, no. 5, pp. 65–74, 2018.
- [2] J. B. Neris, F. H. M. Luzardo, E. G. P. da Silva, and F. G. Velasco, "Evaluation of adsorption processes of metal ions in multi-element aqueous systems by lignocellulosic adsorbents applying different isotherms: A critical review," *Chem. Eng. J.*, vol. 357, pp. 440–420, 2019. DOI: 10.1016/j.cej.2018.09.125
- [3] M. Manjuladevi, R. Anitha, and S. Manonmani, "Kinetic study on adsorption of Cr (VI), Ni (II), Cd (II) and Pb (II) ions from aqueous solutions using activated carbon prepared from Cucumis melo peel," *Appl. Water Sci.*, vol. 8, no. 1, p. 36, 2018. DOI: 10.1007/s13201-018-0674-1
- [4] J. Long, X. Huang, X. Fan, Y. Peng, and J. Xia, "Effective adsorption of nickel (II) with *Ulva lactuca* dried biomass: isotherms, kinetics and mechanisms," *Water Sci. Technol.*, vol. 78, no. 1, pp. 1–9, 2018. DOI: 10.2166/wst.2018.253
- [5] C. Tejada-Tovar, A. Herrera-Barros, and A. Villabona-Ortíz, "Assessment of Chemically Modified Lignocellulose Waste for the Adsorption of Cr (VI)," *Rev. Fac. Ing.*, vol. 29, no. 54, p. e10298, 2020. DOI: 10.19053/01211129.v29.n54.2020.10298
- [6] C. Tejada-Tovar, Á. Villabona-Ortíz, and M. Jiménez-Villadiego, "Remoción de cromo hexavalente sobre residuos de cacao pretratados químicamente," *Rev. UDCA Actual. Divulg. Científica*, vol. 10, no. 1, pp. 139–147, 2017.
- [7] E. Duarte, J. Olivero-Verbel, and B. Jaramillo, "Remoción de Cromo de aguas residuales de curtientes usando quitosano obtenido de desechos de camarón," *Sci. Tech.*, vol. 2, no. 42, pp. 290–295, 2009. DOI: 10.22517/23447214.2679
- [8] D. L. Gómez-Aguilar, J. P. Rodríguez-Miranda, J. A. Esteban-Muñoz, and J. F. Betancur, "Coffee Pulp: A Sustainable Alternative Removal of Cr (VI) in Wastewaters. Processes," *Processes*, vol. 7, no. 7, p. 403, 2019. DOI: 10.3390/pr7070403
- [9] A. Kumar *et al.*, "Remediation techniques applied for aqueous system contaminated by toxic Chromium and Nickel ion," *Geol. Ecol. Landscapes*, vol. 1, no. 2, pp. 143–153, 2017. DOI: 10.1080/24749508.2017.1332860
- [10] B. A. Bhavase, R. P. Ugwekar, and R. B. Mankar, *Novel Water Treatment and Separation Methods : Simulation of Chemical Processes*. Waretown: Apple Academic Press, INC, 2017.
- [11] C. Tejada, A. Herrera, and E. Ruiz, "Cinética e isotermas de bioadsorción de Hg (II) usando materiales residuales tratados con ácido cítrico," *Ing. y Competitividad*, vol. 18, no. 1, pp. 117–127, 2016.
- [12] Ş. Parlaklıci and E. Pehlivan, "Comparative study of Cr (VI) removal by bio-waste adsorbents: equilibrium, kinetics, and thermodynamic," *J. Anal. Sci. Technol.*, vol. 10, no. 1, p. 15, 2019. DOI: 10.1186/s40543-019-0175-3
- [13] S. Berhe, D. Ayele, A. Tadesse, and A. Mulu, "Adsorption Efficiency of Coffee Husk for Removal of Lead (II) from Industrial Effluents: Equilibrium and Kinetic Study," *Int. J. Sci. Res. Publ.*, vol. 5, no. 9, pp. 753–859, 2015.
- [14] Y. Yi, J. Lv, Y. Liu, and G. Wu, "Synthesis and application of modified Litchi peel for removal of hexavalent chromium from aqueous solutions," *J. Mol. Liq.*, vol. 225, pp. 28–33, 2017. DOI: 10.1016/j.molliq.2016.10.140
- [15] Y. Chen, H. Wang, W. Zhao, and S. Huang, "Four different kinds of peels as adsorbents for the removal of Cd (II) from aqueous solution: Kinetics, isotherm and mechanism," *J. Taiwan Inst. Chem. Eng.*, vol. 88, pp. 146–151, 2018. DOI: 10.1016/j.jtice.2018.03.046
- [16] L. A. Romero-Cano, H. García-Rosero, L. V. Gonzalez-Gutierrez, L. A. Baldenegro-Pérez, and F. Carrasco-Marín, "Functionalized adsorbents prepared from fruit peels: Equilibrium, kinetic and thermodynamic studies for copper adsorption in aqueous solution," *J. Clean. Prod.*, 2017. DOI: 10.1016/j.jclepro.2017.06.032
- [17] R. Sudha, K. Srinivasan, and P. Premkumar, "Removal of Nickel (II) from aqueous solution using Citrus Limettoides peel and seed carbon," *Ecotoxicol. Environ. Saf.*, vol. 117, pp. 115–123, 2015. DOI: 10.1016/j.ecoenv.2015.03.025
- [18] C. N. Tejada-Tovar, Z. Montiel, and D. Acevedo, "Aprovechamiento de Cáscaras de Yuca y Ñame para el Tratamiento de Aguas Residuales Contaminadas con Pb(II)," *Inf. Tecnol.*, 2016.
- [19] D. Sivakumar, D. Shankar, R. Mahalakshmi, and K. Deepalakshmi, "Kinetic Model Studies on Removal of Hexavalent Chromium-Sugarcane Bagasse Powder," *Int. Res. J. Multidiscip. Sci. Technol.*, vol. 2, no. 5, pp. 37–43, 2017.
- [20] O. M. Rodriguez-Narvaez, J. M. Peralta-Hernandez, A. Goonetilleke, and E. R. Bandala, "Treatment technologies for emerging contaminants in water: A review," *Chem. Eng. J.*, vol. 323, pp. 361–380, Sep. 2017. DOI: 10.1016/j.cej.2017.04.106
- [21] N. P. Raval, P. U. Shah, and N. K. Shah, "Adsorptive removal of nickel (II) ions from aqueous environment: A review," *J. Environ. Manage.*, vol. 179, pp. 1–20, 2016. DOI: 10.1016/j.jenvman.2016.04.045
- [22] S. Afroze and T. K. Sen, "A Review on Heavy Metal Ions and Dye Adsorption from Water by Agricultural Solid Waste Adsorbents," *Water, Air Soil Pollut.*, vol. 229, no. 7, p. 225, 2018. DOI: 10.1007/s11270-018-3869-z
- [23] A. Azimi, A. Azari, M. Rezakazemi, and M. Ansarpour, "Removal of heavy metals from industrial wastewaters: A Review," *ChemBioEng Rev.*, vol. 4, no. 1, pp. 37–59, 2017. DOI: 10.1002/cben.201600010
- [24] J. Lara, C. Tejada-Tovar, A. Villabona-Ortíz, and A. Arrieta, "Adsorción de plomo y cadmio en sistema continuo de lecho fijo sobre residuos de cacao," vol. 29, no. 2, pp. 111–122, 2016.
- [25] P. S. Blanes *et al.*, "Application of soy hull biomass in removal of Cr(VI) from contaminated waters. Kinetic, thermodynamic and continuous sorption studies," *J. Environ. Chem. Eng.*, vol. 4, no. 1, pp. 516–526, 2016. DOI: 10.1016/j.jece.2015.12.008
- [26] C. Tejada-Tovar, A. González-Delgado, and A. Villabona-Ortíz, "Characterization of Residual Biomasses and Its Application for the Removal of Lead Ions from Aqueous Solution," *Appl. Sci.*, vol. 9, no. 21, p. 4486, 2019. DOI: 10.3390/app9214486
- [27] N. Medellin-Castillo, "Bioadsorción de plomo (II) presente en solución acuosa sobre residuos de fibras naturales procedentes de la industria ixlera (Agave lechuguilla Torr. y Yucca carnerosana (TREL.) MCKELVEY)," *Rev. Int. Contam. Ambient.*, vol. 33, no. 2, pp. 269–280, 2017. DOI: 10.20937/rica.2017.33.02.08
- [28] R. M. Naik, S. Ratan, and I. Singh, "Use of orange peel as an adsorbent for the removal of Cr (VI) from its aqueous solution," *Indian J. Chem. Technol.*, vol. 25, no. 3, pp. 300–305, 2018.
- [29] S. M. Batagarawa and A. K. Ajibola, "Comparative evaluation for the adsorption of toxic heavy metals on to millet, corn and rice husks as adsorbents," *J. Anal. Pharm. Res.*, vol. 8, no. 3, pp. 119–125, 2019. DOI: 10.15406/japlr.2019.08.00325
- [30] D. Cherik and K. Louhab, "A kinetics, isotherms, and thermodynamic study of diclofenac adsorption using activated carbon prepared from olive stones," *J. Dispers. Sci. Technol.*, vol. 39, no. 6, pp. 814–825, 2018. DOI: 10.1080/01932691.2017.1395346
- [31] V. Manirethan, N. Gupta, R. M. Balakrishnan, and K. Raval, "Batch and continuous studies on the removal of heavy metals from aqueous solution using biosynthesised melanin-coated PVDF membranes," *Environ. Sci. Pollut. Res.*, pp. 1–15, 2019. DOI: 10.1007/s11356-019-06310-8
- [32] C. Tejada-Tovar, A. Villabona-Ortíz, and E. Ruiz-Paternina, "Cinética de adsorción de Cr (VI) usando biomasas residuales modificadas químicamente en sistemas por lotes y continuo," *Rev. Ion*, vol. 28, no. 1, pp. 29–41, 2015.
- [33] C. Tejada-Tovar, A. Villabona-Ortíz, Á. D. González-Delgado, C. Granados-Conde, and M. Jiménez-Villadiego, "Kinetics of Mercury and Nickel adsorption using chemically pretreated cocoa (*Theobroma cacao*) husk," *Trans. ASABE*, vol. 62, no. 2, pp. 461–466, 2019. DOI: 10.13031/trans.13133
- [34] X. Luo, Y. Cai, L. Liu, and J. Zeng, "Cr (VI) adsorption performance and mechanism of an effective activated carbon prepared from bagasse with a one-step pyrolysis and ZnCl₂ activation method," *Cellulose*, vol. 26, no. 8, pp. 4921–4934, 2019. DOI: 10.1007/s10570-019-02418-9
- [35] E. D. Asuquo and A. D. Martin, "Sorption of cadmium (II) ion from aqueous solution onto sweet potato (*Ipomoea batatas* L.) peel adsorbent: Characterisation, kinetic and isotherm studies," *J. Environ. Chem. Eng.*, 2016. DOI: 10.1016/j.jece.2016.09.024
- [36] S. Ratan, I. Singh, J. Sarkar, and N. Rm, "The Removal of Nickel from Waste Water by Modified Coconut Coir Pith," *Chem. Sci. J.*,

- vol. 7, no. 3, pp. 1–6, 2016. DOI: 10.4172/2150-3494.1000136
- [37] C. Tejada, A. Villabona, and E. Ruiz, "Adsorción de NI (ii) por cáscaras de ñame (*Discorea rotundata*) y Bazago de Palma (*Elaeis guineensis*) Pretratadas," *Luna Azul*, no. 42, pp. 30–43, 2016.
- [38] N. M. A. Al-Lagtaah, A. H. Al-Muhtaseb, M. N. M. Ahmad, and Y. Salameh, "Chemical and physical characteristics of optimal synthesised activated carbons from grass-derived sulfonated lignin versus commercial activated carbons," *Microporous Mesoporous Mater.*, vol. 225, pp. 504–514, 2016.
- [39] H. N. Tran, S. J. You, and H. P. Chao, "Thermodynamic parameters of cadmium adsorption onto orange peel calculated from various methods: A comparison study," *J. Environ. Chem. Eng.*, vol. 4, no. 3, pp. 2671–2682, 2016. DOI: 10.1016/j.jece.2016.05.009
- [40] Y. Miguel-Gallo, I. Rodríguez Rico, and J. Prieto García, "Influencia del pH y la temperatura en la adsorción de fenol en agua utilizando ceniza de bagazo de caña de azúcar," *Afinidad Rev. química teórica y Apl.*, vol. 74, no. 579, pp. 176–179, 2017.
- [41] M. Akram, H. N. Bhatti, M. Iqbal, S. Noreen, and S. Sadaf, "Biocomposite efficiency for Cr(VI) adsorption: Kinetic, equilibrium and thermodynamics studies," *Biochem. Pharmacol.*, vol. 5, no. 1, pp. 400–411, 2016. DOI: 10.1016/j.jece.2016.12.002
- [42] P. Premkumar and R. Sudha, "Comparative studies on the removal of chromium (VI) from aqueous solutions using raw and modified Citrus Limettoides peel," *Indian J. Chem. Technol.*, vol. 25, no. 3, pp. 255–265, 2018.
- [43] H. Haroon *et al.*, "Equilibrium kinetic and thermodynamic studies of Cr(VI) adsorption onto a novel adsorbent of Eucalyptus camaldulensis waste: Batch and column reactors," *Korean J. Chem. Eng.*, vol. 33, no. 10, pp. 2898–2907, 2016. DOI: 10.1016/j.molliq.2017.04.029
- [44] A. Mishra, B. Dutt, and A. Kumar, "Packed-bed column biosorption of chromium (VI) and nickel (II) onto Fenton modified *Hydrilla verticillata* dried biomass," *Ecotoxicol. Environ. Saf.*, vol. 132, pp. 420–428, 2016. DOI: 10.1016/j.ecoenv.2016.06.026
- [45] W. C. Tsai, M. D. G. De Luna, H. L. P. Bermillo-Arriegado, C. M. Futalan, J. I. Colades, and M. W. Wan, "Competitive Fixed-Bed Adsorption of Pb(II), Cu(II), and Ni(II) from Aqueous Solution Using Chitosan-Coated Bentonite," *Int. J. Polym. Sci.*, vol. 2016, no. II, 2016. DOI: 10.1155/2016/1608939
- [46] J. L. Gong *et al.*, "Continuous adsorption of Pb(II) and methylene blue by engineered graphite oxide coated sand in fixed-bed column," *Appl. Surf. Sci.*, vol. 330, pp. 148–157, 2015. DOI: 10.1016/j.apsusc.2014.11.068
- [47] S. Muthusaravanan *et al.*, "Phytoremediation of heavy metals: mechanisms, methods and enhancements," *Environ. Chem. Lett.*, vol. 16, no. 4, pp. 1339–1359, 2018. DOI: 10.1007/s10311-018-0762-3
- [48] Z. Z. Chowdhury, S. M. Zain, A. K. Rashid, R. F. Rafique, and K. Khalid, "Breakthrough curve analysis for column dynamics sorption of Mn(II) ions from wastewater by using Mangostana garcinia peel-based granular-activated carbon," *J. Chem.*, vol. 2013, 2013. DOI: 10.1155/2013/959761
- [49] J. S. Valencia Ríos and G. C. Castellar Ortega, "Predicción de las curvas de ruptura para la remoción de Plomo (II) en disolución acuosa sobre carbón activado en una columna empacada," *Rev. Fac. Ing.*, vol. 66, pp. 141–158, 2013.
- [50] S. Amirnia, M. B. Ray, and A. Margaritis, "Copper ion removal by Acer saccharum leaves in a regenerable continuous-flow column," *Chem. Eng. J.*, vol. 287, pp. 755–764, 2016. DOI: 10.1016/j.cej.2015.11.056
- [51] S. Vilvanathan and S. Shanthakumar, "Column adsorption studies on Nickel and Cobalt removal from aqueous solution using native and biochar form of *Tectona grandis*," *Environ. Prog. Sustain. Energy*, vol. 35, no. 3, pp. 809–814, 2015. DOI: 10.1002/ep.12567
- [52] A. ul Haq, M. Saeed, S. Anjum, T. H. Bokhari, M. Usman, and S. Tubbs, "Evaluation of Sorption Mechanism of Pb (II) and Ni (II) onto Pea (*Pisum sativum*) Peels," *J. Oleo Sci.*, vol. 743, no. 7, pp. 735–743, 2017. DOI: 10.5650/jos.ess17020
- [53] H. Guedidi, L. Reinert, Y. Soneda, N. Bellakhal, and L. Duclaux, "Adsorption of ibuprofen from aqueous solution on chemically surface-modified activated carbon cloths," *Arab. J. Chem.*, vol. 10, pp. S3584–S3594, 2017. DOI: 10.1016/j.arabjc.2014.03.007
- [54] X. Fan, J. Xia, and J. Long, "The Potential of Nonliving *Sargassum hemiphyllum* as a Biosorbent for Nickel (II) Removal — Isotherm, Kinetics, and Thermodynamics Analysis," *Environ. Prog. Sustain. Energy*, vol. 38, no. S1, pp. S250–S259, 2018. DOI: 10.1002/ep.12997
- [55] S. Mondal, K. Sinha, K. Aikat, and G. Halder, "Adsorption

thermodynamics and kinetics of ranitidine hydrochloride onto superheated steam activated carbon derived from mung bean husk," *J. Environ. Chem. Eng.*, vol. 3, no. 1, pp. 187–195, 2015. DOI: 10.1016/j.jece.2014.11.021



Candelaria Tejada-Tovar She is a Chemical Engineer from the Industrial University of Santander. Specialist in Analytical Chemistry and Master in Environmental Engineering from the University of Cartagena. She has been a research

professor in the Chemical Engineering program at the University of Cartagena since 2006, and is an Associate Researcher at COLCIENCIAS of the Process Design and Biomass Utilization Research Group (IDAB). Her research interests include water treatment, biomass utilization, waste recovery, and environmental engineering.

ORCID: <https://orcid.org/0000-0002-2323-1544>



Luis Newball López He is a Chemical Engineer from the Universidad de Cartagena; of the Process Design and Biomass Utilization Research Group (IDAB). Her research interests include water treatment, biomass utilization, waste recovery, and environmental engineering.

ORCID: <https://orcid.org/0000-0002-6789-0189>



Camilo Cardona Lara He is a Chemical Engineer from the Universidad de Cartagena; of the Process Design and Biomass Utilization Research Group (IDAB). Her research interests include water treatment, biomass utilization, waste recovery, and environmental engineering.

ORCID: <https://orcid.org/0000-0002-0673-6284>